

Probing globular clusters using modulated gravitational waves from binary black holes

Jie Wu^{1,3}, Yao Xiao², Mengfei Sun^{1,3}, Jin Li^{1,3,4*}

¹College of Physics, Chongqing University, Chongqing, 401331, China.

²South-Western Institute for Astronomy Research, Yunnan University, Kunming, 650500, China.

³Department of Physics and Chongqing Key Laboratory for Strongly Coupled Physics, Chongqing University, Chongqing, 401331, China.

⁴Institute of Advanced Interdisciplinary Studies, Chongqing University, Chongqing, 401331, China.

*Corresponding author(s). E-mail(s): cqujinli1983@cqu.edu.cn;

Abstract

Globular clusters (GCs) are crucial for studying stellar dynamics and galactic structure, yet precise measurements of their distances and masses are often limited by uncertainties in electromagnetic (EM) observations. We present a novel method that leverages gravitational waves (GWs) from stellar-mass binary black holes (BBHs) orbiting within GCs to enhance the precision of GC parameter measurements. The BBH's orbital motion imprints characteristic modulations on the GW waveform, encoding information about the host GC. Using post-Newtonian waveforms and Lorentz transformations, we simulate modulated GW signals and evaluate the resulting parameter constraints via a Fisher information matrix analysis. Our results show that incorporating GW observations can significantly reduce the uncertainties in GC distance and mass measurements, in many cases achieving improvements by an order of magnitude. These findings demonstrate the value of BBHs as dynamical probes and highlight the power of GWs to advance GC studies beyond the limits of traditional EM methods.

1 Introduction

Globular clusters (GCs) are among the oldest stellar systems in the Universe. They typically consist of dense, gravitationally bound collections of about $10^4 - 10^6$ stars,

serving as important laboratories for studying stellar evolution, galaxy formation, and cosmology [1]. Because of their longevity and widespread presence in galaxies, GCs provide critical insights into the formation histories of their hosts, making them key tracers of galaxy evolution and cosmic structure assembly [2, 3].

Precise measurements of GC distances and masses are of particular importance. Accurate determinations of GC distances are fundamental for establishing the astronomical distance scale. They serve as valuable calibration points for standard candles and help improve extinction corrections within the Milky Way and nearby galaxies [4, 5]. High-precision GC distance measurements thus play a vital role in mapping cosmic structures, refining the cosmic distance ladder, and constraining cosmological parameters such as the Hubble constant [6, 7]. Likewise, accurately determining GC masses is essential for understanding their internal dynamics, formation mechanisms, and subsequent evolution. Mass measurements reveal core collapse phenomena, mass segregation, and stellar interactions within GCs, thereby refining theoretical models of their long-term evolution [8]. Furthermore, GC mass distributions provide insight into dark matter content and stellar populations, highlighting the interplay between internal dynamics and the external galactic environment [9, 10].

Given these motivations, enhancing the precision of GC distance and mass measurements remains an active and important area of research in astrophysics. However, current methods for determining GC distances and masses primarily rely on electromagnetic (EM) observations. Distances are commonly determined using standard candles (e.g., RR Lyrae stars and Type II Cepheids) or via trigonometric parallaxes [11, 12]. Masses are typically inferred from dynamical models based on velocity dispersion measurements or surface brightness profiles [13, 14]. Although these techniques have led to significant progress, they remain limited by factors such as dust extinction, line-of-sight projection effects, and assumptions of dynamical equilibrium [15]. These limitations motivate the development of alternative and independent approaches to improve the precision of GC parameter measurements.

Since the first detection of gravitational waves (GWs) in 2015, GW astronomy has rapidly grown into a transformative field, offering a fundamentally different observational perspective compared to traditional EM methods [16, 17]. A major advantage of GW signals is their immunity to dust extinction and line-of-sight projection effects, enabling robust detection even in crowded or obscured regions [18, 19]. Among various GW sources, stellar-mass binary black holes (BBHs) stand out as the most prominent and best-studied population to date [20]. Most GW events detected so far originate from BBH mergers, making BBHs the most common and observationally accessible GW sources [21]. The waveform properties of BBHs have been extensively analyzed for a broad range of masses and orbital configurations, providing a solid foundation for extracting astrophysical parameters from GW signals [22]. These properties make BBHs powerful tools for providing independent constraints on GC distances and masses via GW observations.

The potential of using BBHs to probe GCs has already been explored in several earlier studies, laying the groundwork for subsequent developments. Rodriguez *et al.* and Kremer *et al.* investigated the detectability of BBHs originating in GCs using ground-based facilities (e.g., LIGO) and space-based observatories (e.g., LISA) [23, 24]. Their

results confirmed that such systems are likely to be detectable with both current and future detectors. Stokov *et al.* proposed measuring the Doppler shift induced by a BBH’s radial motion as a method to detect intermediate-mass black holes in clusters [25]. Tiwari *et al.* showed that the line-of-sight acceleration of a BBH (detectable by space-based detectors such as DECIGO and LISA) can be used to infer the physical properties of its host cluster [26]. In a related study, Stegmann *et al.* found that when stellar-mass BBHs orbit supermassive black hole binaries (SMBHBs), the BBHs’ motion can imprint characteristic modulations on decihertz GW signals [27]. Such modulation features enable population studies of SMBHBs through detailed waveform analysis. Collectively, these studies exploit how the orbital motion of BBHs around massive objects influences GW signals, underscoring a promising approach to probing cluster parameters via detailed waveform analysis.

In this work, we present a novel GW-based method for probing GCs. Specifically, we examine how the orbital motion of a stellar-mass BBH within a GC modulates its GW signal through waveform transformations derived from Lorentz boosts. These transformations capture the effects of BBHs orbiting within the GC and enable constraints on the host GC’s distance and mass. By applying a Fisher information matrix (FIM) analysis to GW signals, we quantify the uncertainties in GC parameters achievable with LISA observations and compare these with existing EM constraints. This allows us to assess the improvement from combining GW and EM measurements in a multi-messenger framework. A key innovation of our approach is the implementation of full waveform transformations that account for arbitrary source motion directions, going beyond previous treatments that were limited to line-of-sight velocity and edge-on orbital configurations, neglecting the effect of transverse motion. The GW signals used in this study are simulated using second-generation time-delay interferometry (TDI), ensuring consistency with future space-based GW observations. Furthermore, we construct asymmetric normal distributions based on existing EM observations to model the combined parameter distributions from EM and GW data, allowing us to assess the theoretical potential of multi-messenger constraints. Overall, these developments offer a new perspective and methodology for GC studies.

2 Results

2.1 GW modulation

For BBH systems in the rest frame, the GWs observed by a space-based detector like LISA correspond to the early inspiral phase. During this phase, the waveform’s amplitude and frequency evolve slowly, such that post-Newtonian (PN) models are particularly well-suited for accurate waveform modeling. However, if the BBH is orbiting within a GC, this motion induces periodic changes in the waveform, imprinting characteristic modulation features on the observed signal.

As illustrated in Fig. 1, the waveform of a moving BBH source differs significantly from that of a rest BBH. In the frequency domain, modulation gives rise to sidebands surrounding the central spectral peak. These sidebands are separated by integer multiples of the inverse outer orbital period, forming a regular structure that reflects the

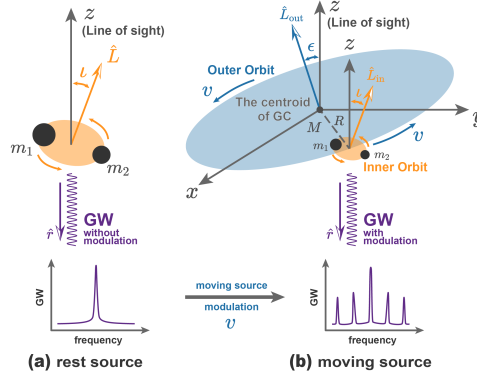


Fig. 1 Schematic illustration of GW modulation. Panel (a) depicts a BBH at rest with respect to the observer, emitting an unmodulated GW signal. Panel (b) shows a BBH moving in an outer orbit around the GC’s centroid, which introduces periodic modulation in the observed GW signal. In both cases, the lower sub-panels present simplified representations of the corresponding GW frequency spectra. This figure is for conceptual illustration only and does not represent actual spatial scales or the full complexity of the waveform used in our analysis.

periodic nature of the source’s motion. These features serve as direct signatures of the source’s orbital dynamics, encoding information about the host GC.

The presence of such modulation in the waveform provides an additional channel for extracting information from GW observations. Analysis of these modulation features enables us to infer key GC parameters—most notably the GC’s distance and mass. In the following sections, we demonstrate how modulation affects parameter estimation in our analysis.

2.2 Multi-messenger observations

To quantitatively assess the improvements provided by modulated GW signals over traditional EM observations in constraining GC parameters, we employ a FIM analysis to estimate the uncertainties of the relevant GW parameters. This allows us to evaluate the theoretical precision with which these modulation features enable us to infer the properties of the host GC. Based on existing EM measurements, we construct two datasets—EM1 for Milky Way GCs and EM2 for extragalactic GCs—representing the known parameters of these clusters [6, 28]. We then calculate the reduction in parameter uncertainties achieved by incorporating GW observations.

Figure 2 shows the reduction in GC parameter uncertainties after adding GW information to existing EM measurements. These results clearly show that multi-messenger observations significantly enhance the precision of GC parameter estimates. The improvement is most pronounced for Milky Way GCs, with distance uncertainties reduced by up to an order of magnitude for many clusters. In contrast, the improvement for extragalactic GCs is marginal. Specifically, for Milky Way GCs the median relative distance uncertainty decreases from 2.67% (EM1) to 0.27% (EM1+GW). For extragalactic GCs, it decreases only marginally, from 8.43% (EM2) to 8.05% (EM2+GW). This discrepancy arises from the inverse dependence of GW amplitude

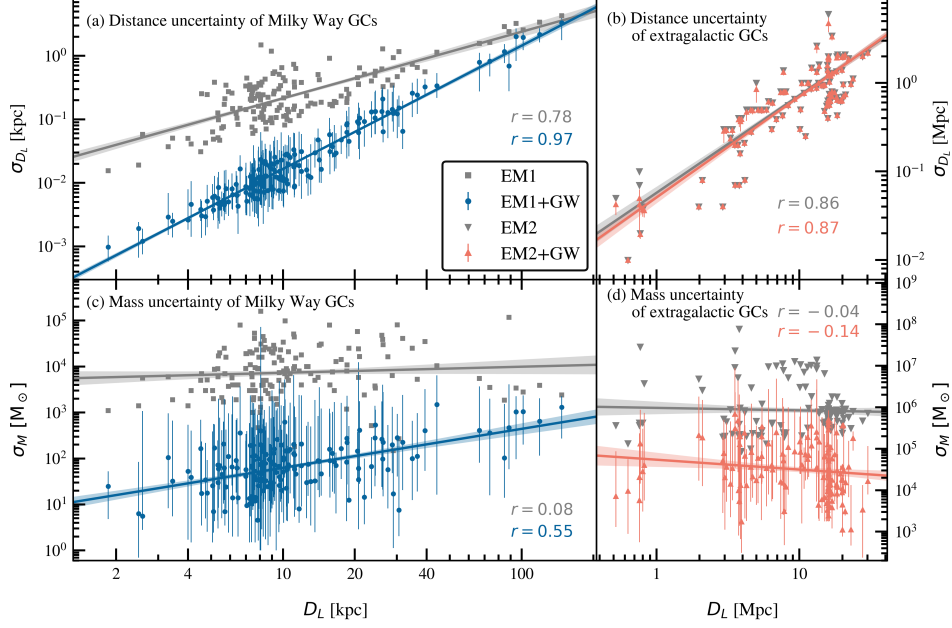


Fig. 2 Relationship between the uncertainty of GC parameters and distance. Panels (a) and (b) show the distance uncertainties for Milky Way and extragalactic GCs, respectively, while panels (c) and (d) show the mass uncertainties. Grey markers represent existing EM-only measurements, and coloured markers denote the results after incorporating GW observations (EM+GW). Vertical bars indicate the 1σ spread in uncertainties arising from different BBH configurations within each GC. The reported value r refers to the Pearson correlation coefficient. Both axes use a logarithmic scale. Solid lines show linear fits to the data in logarithmic space.

on distance [29]. Weaker GW signals from more distant sources carry less information, limiting their effectiveness in constraining host GC parameters.

In comparison, the mass uncertainty exhibits substantial improvement for both Milky Way and extragalactic GCs. In fact, in several cases the uncertainty is reduced by nearly two orders of magnitude. Quantitatively, the median relative mass uncertainty drops from 11.26% to 0.42% for Milky Way GCs. For extragalactic GCs, it declines from 50.09% to 5.45% upon inclusion of the GW data. This enhancement is attributed to the high sensitivity of GWs to frequency evolution [30]. GC mass influences the modulation pattern in a nonlinear and complex way. As a result, the mass uncertainty shows a weaker correlation with distance than observed for the distance uncertainty.

To further investigate the impact of waveform modulation, Figure 3 shows how the relative uncertainties in GC parameters depend on the BBH orbital velocity. A clear negative correlation is observed: as the velocity increases, the relative uncertainties in both distance and mass decrease. This trend is especially pronounced for mass measurements, which show an even stronger correlation with velocity. Physically, higher orbital velocities enhance the modulation strength of the GW signal [31, 32]. This yields a richer frequency-domain structure characterized by multiple sidebands. These

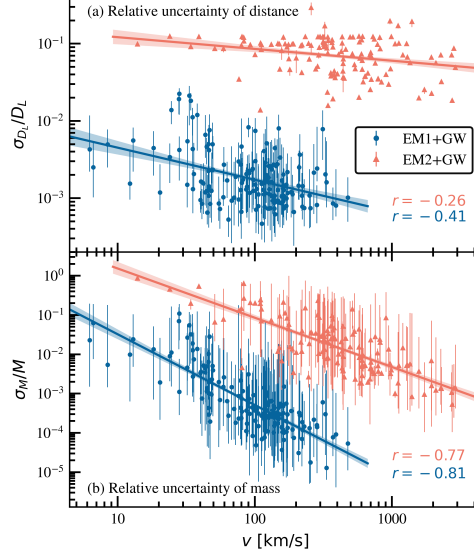


Fig. 3 Relationship between the relative uncertainty of GC parameters and the orbital velocity of BBHs. Panels (a) and (b) show the relative uncertainties in GC distance and mass, respectively. Blue and red markers correspond to multi-messenger observations for Milky Way and extragalactic GCs, respectively. Other plot elements follow the same style as in Fig. 2.

additional features increase the information content of the waveform, enabling more stringent constraints on GC parameters. The effect is more pronounced for Milky Way GCs than for extragalactic GCs, consistent with the weaker GW amplitudes from more distant sources. Given that the orbital velocity scales as $v = \sqrt{GM/R}$, the GC mass M and BBH outer orbital radius R jointly determine the modulation amplitude. These results quantitatively demonstrate the crucial role of waveform modulation in improving the precision of GC distance and mass measurements.

In summary, our findings highlight the potential of GW waveform modulation as a powerful tool for precise GC characterization. Incorporating GW observations into traditional EM frameworks substantially enhances the accuracy of GC distance and mass estimates through multi-messenger measurements. This synergy reduces parameter uncertainties and, in many cases, yields order-of-magnitude improvements in precision beyond what EM-only observations can achieve.

3 Discussion

In this work, we assume that the host GC remains stationary and that the BBH follows a stable outer orbit throughout the observation period. For GW detection, the observation duration is set to one year. Given that the typical proper motion of GCs is on the order of mas/yr, the resulting positional shifts are negligible and do not influence the GW response (as it is computed based on the source’s sky location) [33]. Although the radial velocity of a GC can be comparable in magnitude to the BBH’s orbital velocity, it remains effectively constant in both direction and speed [34, 35]. As

a result, it induces only a static phase offset in the GW waveform—degenerate with the initial phase—and thus does not lead to any modulation [31, 36].

On longer timescales, several astrophysical processes—such as Lense-Thirring precession, Lidov-Kozai oscillations, and dynamical friction from ambient gas—could potentially alter the outer orbit [37–39]. However, these effects typically operate on timescales ranging from thousands to millions of years, far exceeding the duration of observation [40]. Therefore, the assumption of a stable outer orbit is well justified and enables a tractable yet physically meaningful model for our analysis.

Building on these assumptions, we employed a FIM analysis to estimate the parameter uncertainties of BBHs in GCs using GW observations. Combined with existing EM measurements, we constructed asymmetric normal likelihoods to model the joint EM+GW constraints in a multi-messenger framework. This establishes a complete methodology for using BBH-generated GWs as dynamical probes to infer GC distance and mass. Our results demonstrate that this approach can substantially reduce parameter uncertainties compared with using EM observations alone.

It is important to note that the GW-based constraints presented in this study are derived from theoretical estimates using the FIM. Our aim is to theoretically validate the feasibility of this method. Due to the high computational cost of Bayesian inference involving a 13-dimensional parameter space, we did not carry out a full posterior analysis. In the future, we plan to carry out such analyses using real space-based GW data. This will allow us to further test the practical viability of this technique and eventually perform full Bayesian inference to extract GC properties from GW signals.

4 Methods

4.1 GW signal

In this work, we focus on GWs from stellar-mass BBHs within the LISA sensitivity band. These systems are typically tens to thousands of years away from merger. Their inner orbits evolve slowly over observational timescales, making them well-suited for waveform modeling using PN methods. We adopt the 3.5PN formalism, including both spin-orbit and spin-spin couplings, to generate inspiral waveforms in the rest frame of the BBH [30, 41, 42].

Within four-dimensional spacetime, GWs are characterized by having boost weight zero and spin weight 2, making full Lorentz transformations difficult [36]. However, due to the transverse-traceless requirement, GWs can be effectively described using three-dimensional spatial tensors. This allows frame transformations to be implemented through a combination of three-dimensional Lorentz tensor transformations and time coordinate rescaling. A complete derivation of this formalism can be found in Ref. [36]. Under this approach, the GW signal h_{ij} in a frame moving at an arbitrary velocity \vec{v}

(in natural units where $c = 1$) relative to the rest frame can be expressed as

$$\begin{aligned}
h'_{ij} = & h_{ij} + v^k h_{kl} v^l \frac{1}{(1 - \hat{r} \cdot \vec{v})^2} [\hat{r}_i \hat{r}_j \\
& - \frac{\gamma}{1 + \gamma} (\hat{r}_i v_j + v_i \hat{r}_j) + \frac{\gamma^2}{(1 + \gamma)^2} v_i v_j] \\
& + v^k h_{kj} \frac{1}{1 - \hat{r} \cdot \vec{v}} [\hat{r}_i - \frac{\gamma}{1 + \gamma} v_i] \\
& + v^k h_{ik} \frac{1}{1 - \hat{r} \cdot \vec{v}} [\hat{r}_j - \frac{\gamma}{1 + \gamma} v_j],
\end{aligned} \tag{1}$$

$$h'_{ij}(t) = h'_{ij}(t' \gamma (1 - \vec{v} \cdot \hat{r})), \tag{2}$$

where $\gamma = 1/\sqrt{1 - v^2}$ is the Lorentz factor, \hat{r} denotes the propagation direction of the GW. This formulation enables us to incorporate the velocity arising from the BBH's orbital motion around the GC into the waveform.

Following this transformation, we compute the LISA detector response to the modulated waveform over a one-year observation period, which matches LISA's orbital period. We employ a realistic simulation pipeline that incorporates TDI techniques. In this pipeline, we use second-order eccentric Keplerian orbits to model LISA's motion, allowing for unequal arm lengths that vary over time. The resulting TDI 2.0 Michelson-type data stream is constructed across the X , Y , and Z channels. Full details of the response implementation can be found in Ref. [43].

4.2 GC data

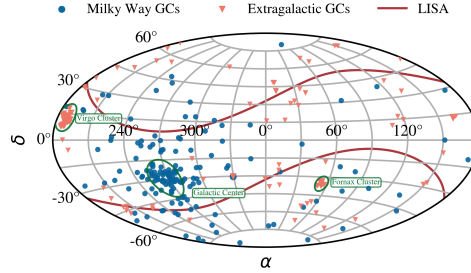


Fig. 4 Sky locations of selected GCs from EM observations. Blue markers show the positions of Milky Way GCs, and red markers show those of extragalactic GCs. The solid red curve indicates the annual trajectory of the normal vector of the LISA constellation plane.

The GC parameters adopted in this study are drawn from multiple EM observational sources, including measurements from the *Hubble Space Telescope* and *Gaia*. From Refs. [6, 28], we extract key GC properties, including the GC mass M , luminosity distance D_L , and sky location (right ascension α and declination δ). The spatial

distribution of the selected GCs is illustrated in Fig. 4, with Milky Way GCs clustering around the Galactic Center and extragalactic GCs located primarily in the Virgo and Fornax clusters.

For BBH properties, we utilize simulation data from Ref. [44], which provides a catalog of large-scale cluster Monte Carlo (CMC) simulations. These simulations, based on the Hénon-type Monte Carlo algorithm, incorporate a wide range of physical processes and follow the long-term dynamical evolution of dense star clusters. We match each EM-observed GC with a simulated CMC cluster of comparable mass and extract BBH candidates likely to exist in that GC. The parameters extracted include the component masses (m_1 and m_2) and the outer orbital radius (R).

For additional source parameters such as the spin χ and inclination angle ι , we assume uniform sampling over physically motivated ranges, following Ref. [30]. This process yields a comprehensive set of source parameters for waveform modeling and uncertainty estimation. Given the diversity of GC properties and our sampling of stochastic parameters, we assign to each EM-observed GC 20 BBH from the CMC catalog that best match its mass. For each of these BBHs, we compute the corresponding EM+GW constraint and statistically combine the results. Thus, each individual EM measurement in Figs. 2 and 3 corresponds to a distribution of EM+GW results.

4.3 Data analysis

After generating the parameter dataset, we compute the corresponding GW waveform for each BBH source and then perform data analysis to evaluate the associated uncertainties in the GC parameters. The complete analysis pipeline is illustrated in Fig. 5.

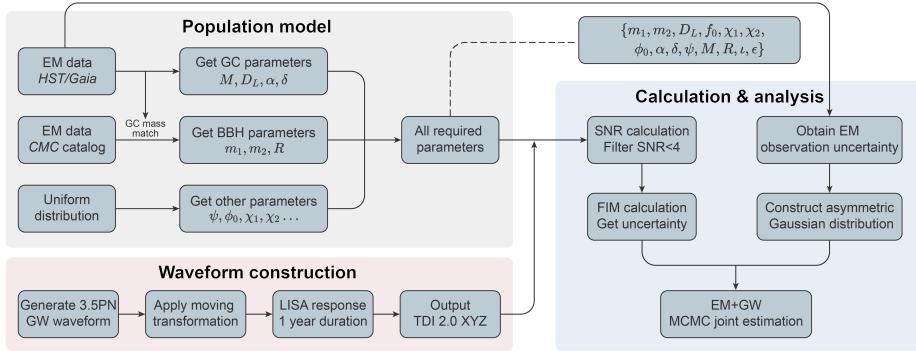


Fig. 5 Schematic workflow of the data generation and analysis process. The pipeline consists of three main components: population modelling (top-left), waveform construction (bottom), and uncertainty estimation (right).

The analysis begins with computing the signal-to-noise ratio (SNR) for each sample. We exclude any source with $\text{SNR} < 4$, as this corresponds to an effective detection

threshold of $\text{SNR} = 8$ for a four-year observation [26, 45]. The SNR is given by [46]

$$\text{SNR} = \sqrt{(h|h)}, \quad (3)$$

where the inner product $(a|b)$ is defined as

$$(a|b) = 4 \text{Re} \int_0^\infty \frac{\tilde{a}^*(f) \tilde{b}(f)}{S_n(f)} df, \quad (4)$$

where $S_n(f)$ is the one-sided power spectral density of the detector noise, and $\tilde{a}(f)$ and $\tilde{b}(f)$ are the Fourier transforms of $a(t)$ and $b(t)$, respectively. For each detectable source, we estimate parameter uncertainties using the FIM, defined as [47]

$$\Gamma_{ij} = \left(\frac{\partial h}{\partial \theta_i} \middle| \frac{\partial h}{\partial \theta_j} \right), \quad (5)$$

where θ_i denotes the i -th parameter in the waveform model. The inverse of the Γ yields the parameter covariance matrix, and the 1σ uncertainty in θ_i is given by $\sigma_{\text{GW } i} = \sqrt{(\Gamma^{-1})_{ii}}$.

To further improve the measurement precision of GC parameters, we incorporate both GW and existing EM measurements into a unified statistical framework. Since many EM-based uncertainties are significantly asymmetric, we model them using asymmetric normal distributions $p_{\text{EM}}(\theta)$ that provide a more faithful representation of the observational results [48]. Based on the uncertainties σ_{GW} derived from the FIM, we construct a corresponding normal distribution $p_{\text{GW}}(\theta)$. The combined effect of EM and GW observations is obtained by multiplying the two distributions, forming a joint distribution $p_{\text{EM+GW}}(\theta) \propto p_{\text{EM}}(\theta) \cdot p_{\text{GW}}(\theta)$. Since the GW constraint provides additional, independent information, the combined distribution is always narrower than the original EM distribution, resulting in EM+GW error bars that lie strictly below the EM-only points in Fig. 2.

We then employ a Markov Chain Monte Carlo (MCMC) algorithm to explore the joint distribution $p_{\text{EM+GW}}(\theta)$ and evaluate the resulting constraints on GC distance and mass. Details of the asymmetric modeling procedure and sampling strategy can be found in Ref. [48].

Collectively, these steps provide a practical and theoretically grounded framework for extracting improved GC parameters via multi-messenger observations.

Acknowledgements. This work was supported by the National Key Research and Development Program of China (Grant No. 2023YFC2206702), the Fundamental Research Funds for the Central Universities Project (Grant No. 2024IAIS-ZD009), the National Natural Science Foundation of China (Grant No. 12347101), and the Natural Science Foundation of Chongqing (Grant No. CSTB2023NSCQ-MSX0103).

Data availability. The EM observational data used in this study are taken from Refs. [6, 28], which provide measurements of globular cluster mass, distance, and sky position. These datasets are publicly available at <https://people>.

smp.uq.edu.au/HolgerBaumgardt/globular/ and <https://vizier.cds.unistra.fr/viz-bin/VizieR-3?-source=J/ApJ/772/82/table1>. The CMC Cluster Catalog is from Ref. [44] and can be accessed at <https://cmc.ciera.northwestern.edu/>.

References

- [1] Benacquista, M.J., Downing, J.M.B.: Relativistic binaries in globular clusters. *Living Rev. Rel.* **16**, 4 (2013) <https://doi.org/10.12942/lrr-2013-4> [arXiv:1110.4423](https://arxiv.org/abs/1110.4423) [astro-ph.SR]
- [2] Forbes, D.A., Bastian, N., Gieles, M., Crain, R.A., Kruijssen, J.M.D., Larsen, S.S., Ploekinger, S., Agertz, O., Trenti, M., Ferguson, A.M.N., Pfeffer, J., Gnedin, O.Y.: Globular cluster formation and evolution in the context of cosmological galaxy assembly: open questions. *Proc. Roy. Soc. Lond. A* **474**, 20170616 (2018) <https://doi.org/10.1098/rspa.2017.0616>
- [3] Meylan, G., Heggie, D.C.: Internal dynamics of globular clusters. *Astron. Astrophys. Rev.* **8**, 1–143 (1997) <https://doi.org/10.1007/s001590050008>
- [4] Rejkuba, M.: Globular cluster luminosity function as distance indicator. *Astrophys. Space Sci.* **341**, 195–206 (2012) <https://doi.org/10.1007/s10509-012-0986-9>
- [5] Chaboyer, B.: Globular cluster distance determinations. In: Heck, A., Caputo, F. (eds.) *Post-Hipparcos Cosmic Candles*, vol. 237. Dordrecht, p. 111 (1999). https://doi.org/10.1007/978-94-011-4734-7_7
- [6] Baumgardt, H., Vasiliev, E.: Accurate distances to galactic globular clusters through a combination of gaia edr3, hst, and literature data. *Mon. Not. Roy. Astron. Soc.* **505**, 5957–5977 (2021) <https://doi.org/10.1093/mnras/stab1474>
- [7] Riess, A.G., Casertano, S., Yuan, W., Bowers, J.B., Macri, L., Zinn, J.C., Scolnic, D.: Cosmic distances calibrated to 1% precision with gaia edr3 parallaxes and hubble space telescope photometry of 75 milky way cepheids confirm tension with Λ CDM. *Astrophys. J. Lett.* **908**, 6 (2021) <https://doi.org/10.3847/2041-8213/abdbaf>
- [8] Baumgardt, H.: N-body modelling of globular clusters: masses, mass-to-light ratios and intermediate-mass black holes. *Mon. Not. Roy. Astron. Soc.* **464**, 2174–2202 (2017) <https://doi.org/10.1093/mnras/stw2488>
- [9] Hudson, M.J., Harris, G.L., Harris, W.E.: Dark matter halos in galaxies and globular cluster populations. *Astrophys. J. Lett.* **787**, 5 (2014) <https://doi.org/10.1088/2041-8205/787/1/L5>
- [10] Harris, W.E., Blakeslee, J.P., Harris, G.L.H.: Galactic dark matter halos and globular cluster populations. iii. extension to extreme environments. *Astrophys. J.* **836**, 67 (2017) <https://doi.org/10.3847/1538-4357/836/1/67>

- [11] Bhardwaj, A.: Rr lyrae and type ii cepheid variables in globular clusters: Optical and infrared properties. *Universe* **8**, 122 (2022) <https://doi.org/10.3390/universe8020122> [arXiv:2202.06982](https://arxiv.org/abs/2202.06982) [astro-ph.SR]
- [12] Vasiliev, E., Baumgardt, H.: Gaiaedr3 view on galactic globular clusters. *Mon. Not. Roy. Astron. Soc.* **505**, 5978–6002 (2021) <https://doi.org/10.1093/mnras/stab1475> [arXiv:2102.09568](https://arxiv.org/abs/2102.09568) [astro-ph.GA]
- [13] Zocchi, A., Bertin, G., Varri, A.L.: A dynamical study of galactic globular clusters under different relaxation conditions. *Astron. Astrophys.* **539**, 65 (2012) <https://doi.org/10.1051/0004-6361/201117977> [arXiv:1201.1466](https://arxiv.org/abs/1201.1466) [astro-ph.GA]
- [14] Baumgardt, H., Côté, P., Hilker, M., Rejkuba, M., Mieske, S., Djorgovski, S.G., Stetson, P.: The velocity dispersion and mass-to-light ratio of the remote halo globular cluster ngc2419. *Mon. Not. Roy. Astron. Soc.* **396**, 2051–2060 (2009) <https://doi.org/10.1111/j.1365-2966.2009.14932.x> [arXiv:0904.3329](https://arxiv.org/abs/0904.3329) [astro-ph.GA]
- [15] Majaess, D., Turner, D., Gieren, W., Lane, D.: The impact of contaminated rr lyrae/globular cluster photometry on the distance scale. *Astrophys. J. Lett.* **752**, 10 (2012) <https://doi.org/10.1088/2041-8205/752/1/L10> [arXiv:1205.0255](https://arxiv.org/abs/1205.0255) [astro-ph.GA]
- [16] Abbott, B.P., *et al.*: Observation of Gravitational Waves from a Binary Black Hole Merger. *Phys. Rev. Lett.* **116**(6), 061102 (2016) <https://doi.org/10.1103/PhysRevLett.116.061102> [arXiv:1602.03837](https://arxiv.org/abs/1602.03837) [gr-qc]
- [17] Bailes, M., *et al.*: Gravitational-wave physics and astronomy in the 2020s and 2030s. *Nat. Rev. Phys.* **3**, 344–366 (2021) <https://doi.org/10.1038/s42254-021-00303-8>
- [18] Hirata, C.M., Holz, D.E., Cutler, C.: Reducing the weak lensing noise for the gravitational wave hubble diagram using the non-gaussianity of the magnification distribution. *Phys. Rev. D* **81**, 124046 (2010) <https://doi.org/10.1103/PhysRevD.81.124046> [arXiv:1004.3988](https://arxiv.org/abs/1004.3988) [astro-ph.CO]
- [19] Colaço, L.R., Holanda, R.F.L., Nunes, R.C., Gonzalez, J.E.: Forecasts analysis on varying- α theories from gravitational wave standard sirens. *Astropart. Phys.* **155**, 102911 (2024) <https://doi.org/10.1016/j.astropartphys.2023.102911>
- [20] Gerosa, D., Fishbach, M.: Hierarchical mergers of stellar-mass black holes and their gravitational-wave signatures. *Nat. Astron.* **5**(8), 749–760 (2021) <https://doi.org/10.1038/s41550-021-01398-w>
- [21] Abbott, R., *et al.*: GWTC-3: Compact Binary Coalescences Observed by LIGO and Virgo during the Second Part of the Third Observing Run. *Phys. Rev. X* **13**(4), 041039 (2023) <https://doi.org/10.1103/PhysRevX.13.041039>

[arXiv:2111.03606](#) [gr-qc]

- [22] Schmidt, P.: Gravitational waves from binary black hole mergers: Modeling and observations. *Front. Astron. Space Sci.* **7** (2020) <https://doi.org/10.3389/fspas.2020.00028>
- [23] Rodriguez, C.L., Morscher, M., Pattabiraman, B., Chatterjee, S., Haster, C.-J., Rasio, F.A.: Binary black hole mergers from globular clusters: Implications for advanced ligo. *Phys. Rev. Lett.* **115**, 051101 (2015) <https://doi.org/10.1103/PhysRevLett.115.051101> [arXiv:1505.00792](#) [astro-ph.HE]
- [24] Kremer, K., Chatterjee, S., Breivik, K., Rodriguez, C.L., Larson, S.L., Rasio, F.A.: Lisa sources in milky way globular clusters. *Phys. Rev. Lett.* **120**, 191103 (2018) <https://doi.org/10.1103/PhysRevLett.120.191103> [arXiv:1802.05661](#) [astro-ph.HE]
- [25] Stokov, V., Fragione, G., Wong, K.W.K., Helfer, T., Berti, E.: Hunting for intermediate-mass black holes with lisa binary radial velocity measurements. *Phys. Rev. D* **105**, 124048 (2022) <https://doi.org/10.1103/PhysRevD.105.124048> [arXiv:2109.08154](#) [astro-ph.HE]
- [26] Tiwari, A., Vijaykumar, A., Kapadia, S.J., Fragione, G., Chatterjee, S.: Accelerated binary black holes in globular clusters: forecasts and detectability in the era of space-based gravitational-wave detectors. *Mon. Not. Roy. Astron. Soc.* **527**, 8586–8597 (2024) <https://doi.org/10.1093/mnras/stad3749> [arXiv:2307.00930](#) [astro-ph.HE]
- [27] Stegmann, J., Zwick, L., Vermeulen, S.M., Antonini, F., Mayer, L.: Imprints of massive black-hole binaries on neighbouring decihertz gravitational-wave sources. *Nat. Astron.* **8**(10), 1321–1331 (2024) <https://doi.org/10.1038/s41550-024-02338-0>
- [28] Harris, W.E., Harris, G.L.H., Alessi, M.: A catalog of globular cluster systems: What determines the size of a galaxy’s globular cluster population? *Astrophys. J.* **772**, 82 (2013) <https://doi.org/10.1088/0004-637X/772/2/82> [arXiv:1306.2247](#) [astro-ph.GA]
- [29] Wu, J., Li, J.: Subtraction of the confusion foreground and parameter uncertainty of resolvable galactic binaries on the networks of space-based gravitational-wave detectors. *Phys. Rev. D* **108**(12), 124047 (2023) <https://doi.org/10.1103/PhysRevD.108.124047> [arXiv:2307.05568](#) [gr-qc]
- [30] Wu, J., Li, J., Liu, X., Cao, Z.: Comparison and application of different post-Newtonian models for inspiralling stellar-mass binary black holes with space-based GW detectors. *Phys. Rev. D* **109**(10), 104014 (2024) <https://doi.org/10.1103/PhysRevD.109.104014> [arXiv:2401.03113](#) [gr-qc]

- [31] Wu, J., Sun, M., Ma, X., Liu, X., Li, J., Cao, Z.: Effect of kick velocity on gravitational wave detection of binary black holes with space- and ground-based detectors. *Phys. Rev. D* **112**(2), 024040 (2025) <https://doi.org/10.1103/2qg3-w39y> [arXiv:2502.13710](https://arxiv.org/abs/2502.13710) [gr-qc]
- [32] Wu, J., Li, J.: Prospects of constraining on the polarizations of gravitational waves from binary black holes using space- and ground-based detectors. *Phys. Rev. D* **110**(8), 084057 (2024) <https://doi.org/10.1103/PhysRevD.110.084057> [arXiv:2407.13590](https://arxiv.org/abs/2407.13590) [gr-qc]
- [33] Vasiliev, E.: Proper motions and dynamics of the milky way globular cluster system from gaia dr2. *Mon. Not. Roy. Astron. Soc.* **484**, 2832–2850 (2019) <https://doi.org/10.1093/mnras/stz171> [arXiv:1807.09775](https://arxiv.org/abs/1807.09775) [astro-ph.GA]
- [34] Forbes, D.A., Alabi, A., Brodie, J.P., Romanowsky, A.J., Strader, J., Foster, C., Usher, C., Spitler, L., Bellstedt, S., Pastorello, N., Villaume, A., Wasserman, A., Pota, V.: The slugs survey: A catalog of over 4000 globular cluster radial velocities in 27 nearby early-type galaxies. *Astron. J.* **153**, 114 (2017) <https://doi.org/10.3847/1538-3881/153/3/114> [arXiv:1701.04835](https://arxiv.org/abs/1701.04835) [astro-ph.GA]
- [35] Baumgardt, H., Hilker, M.: A catalogue of masses, structural parameters, and velocity dispersion profiles of 112 milky way globular clusters. *Mon. Not. Roy. Astron. Soc.* **478**, 1520–1557 (2018) <https://doi.org/10.1093/mnras/sty1057> [arXiv:1804.08359](https://arxiv.org/abs/1804.08359) [astro-ph.GA]
- [36] He, X., Liu, X., Cao, Z.: Lorentz transformation of three dimensional gravitational wave tensor. *Class. Quant. Grav.* **39**(19), 195020 (2022) <https://doi.org/10.1088/1572-9494/acbaeb> [arXiv:2302.07532](https://arxiv.org/abs/2302.07532) [gr-qc]
- [37] Fang, Y., Chen, X., Huang, Q.-G.: Impact of a Spinning Supermassive Black Hole on the Orbit and Gravitational Waves of a Nearby Compact Binary (2019) <https://doi.org/10.3847/1538-4357/ab510e> [arXiv:1908.01443](https://arxiv.org/abs/1908.01443) [astro-ph.HE]
- [38] Ostriker, E.C.: Dynamical friction in a gaseous medium. *Astrophys. J.* **513**, 252 (1999) <https://doi.org/10.1086/306858> [arXiv:astro-ph/9810324](https://arxiv.org/abs/astro-ph/9810324)
- [39] Bartos, I., Kocsis, B., Haiman, Z., Márka, S.: Rapid and Bright Stellar-mass Binary Black Hole Mergers in Active Galactic Nuclei. *Astrophys. J.* **835**(2), 165 (2017) <https://doi.org/10.3847/1538-4357/835/2/165> [arXiv:1602.03831](https://arxiv.org/abs/1602.03831) [astro-ph.HE]
- [40] Yu, H., Chen, Y.: Direct determination of supermassive black hole properties with gravitational-wave radiation from surrounding stellar-mass black hole binaries. *Phys. Rev. Lett.* **126**(2), 021101 (2021) <https://doi.org/10.1103/PhysRevLett.126.021101> [arXiv:2009.02579](https://arxiv.org/abs/2009.02579) [gr-qc]
- [41] Blanchet, L.: Post-Newtonian Theory for Gravitational Waves. *Living Rev. Rel.*

- 17**, 2 (2014) <https://doi.org/10.12942/lrr-2014-2> arXiv:1310.1528 [gr-qc]
- [42] Cho, G., Porto, R.A., Yang, Z.: Gravitational radiation from inspiralling compact objects: Spin effects to the fourth post-Newtonian order. *Phys. Rev. D* **106**(10), 101501 (2022) <https://doi.org/10.1103/PhysRevD.106.L101501> arXiv:2201.05138 [gr-qc]
 - [43] Wu, J., Sun, M., Li, J.: Constraints and detection capabilities of GW polarizations with space-based detectors in different TDI combinations (2024). <https://arxiv.org/abs/2411.03631>
 - [44] Kremer, K., Ye, C.S., Rui, N.Z., Weatherford, N.C., Chatterjee, S., Fragione, G., Rodriguez, C.L., Spera, M., Rasio, F.A.: Modeling Dense Star Clusters in the Milky Way and Beyond with the CMC Cluster Catalog. *Astrophys. J. Suppl.* **247**(2), 48 (2020) <https://doi.org/10.3847/1538-4365/ab7919> arXiv:1911.00018 [astro-ph.HE]
 - [45] Hall, E.D., Evans, M.: Metrics for next-generation gravitational-wave detectors. *Class. Quant. Grav.* **36**(22), 225002 (2019) <https://doi.org/10.1088/1361-6382/ab41d6> arXiv:1902.09485 [astro-ph.IM]
 - [46] Cutler, C.: Angular resolution of the LISA gravitational wave detector. *Phys. Rev. D* **57**, 7089–7102 (1998) <https://doi.org/10.1103/PhysRevD.57.7089> arXiv:gr-qc/9703068
 - [47] Shah, S., Sluys, M., Nelemans, G.: Using electromagnetic observations to aid gravitational-wave parameter estimation of compact binaries observed with LISA. *Astron. Astrophys.* **544**, 153 (2012) <https://doi.org/10.1051/0004-6361/201219309> arXiv:1207.6770 [astro-ph.IM]
 - [48] Possolo, A., Merkatas, C., Bodnar, O.: Asymmetrical uncertainties. *Metrologia* **56**, 045009 (2019) <https://doi.org/10.1088/1681-7575/ab2a8d>